

# Shift and broadening of resonance lines of antiprotonic helium atoms in liquid ${}^4\text{He}$

Andrzej Adamczak\*

*Institute of Nuclear Physics, Polish Academy of Sciences,  
Radzikowskiego 152, PL-31342 Kraków, Poland*

Dimitar Bakalov†

*Institute for Nuclear Research and Nuclear Energy,  
Bulgarian Academy of Sciences, Tsarigradsko chaussée 72, Sofia 1784, Bulgaria*

(Dated: February 26, 2022)

## Abstract

The shift and broadening of the resonance lines in the spectrum of antiprotonic helium atoms  $\bar{p}\text{He}^+$  located in fluid and superfluid  ${}^4\text{He}$  have been estimated. The contributions to the shift and broadening from collective degrees of freedom in liquid  ${}^4\text{He}$  have been evaluated using the phenomenological response function. The shift due to collisions of  $\bar{p}\text{He}^+$  with  ${}^4\text{He}$  atoms has been calculated in the quasistatic limit using the experimental pair-correlation function. It has been shown that an implanted  $\bar{p}\text{He}^+$  atom establishes a good probe of liquid-helium properties, since this atom practically does not change the target structure.

PACS numbers: 36.10.-k, 32.70.Jz, 34.10.+x, 34.20.Cf

---

\*Electronic address: andrzej.adamczak@ifj.edu.pl

†Electronic address: dbakalov@inrne.bas.bg

## I. INTRODUCTION

The exotic antiprotonic helium atoms  $\bar{p}\text{He}^+$  are formed when negatively charged antiprotons are slowed down in helium and later captured by the Coulomb field of the helium nuclei. A fraction of about 3% of the antiprotons are captured in metastable states with lifetimes on the order of microseconds, and this has allowed for a series of high-precision spectroscopy experiments [1] that have produced, among other things, top accuracy values of fundamental particle characteristics such as the electron-to-antiproton mass ratio [2] and the antiproton dipole magnetic moment [3]. These high-accuracy goals required various systematic effects to be accounted for, the density broadening and shift of the spectral lines being among the most important among them [4]. The density effects have been evaluated for a gaseous target in the semiclassical approach [5] using a pairwise interaction potential of an antiprotonic and an ordinary helium atom, calculated *ab initio* in the frame of the symmetrized Rayleigh-Schrödinger theory [6], and the results were in agreement with the experimental data taken at helium gas densities up to 127 g/l [1]. The attempts of the ASACUSA collaboration at CERN for the laser spectroscopy of antiprotonic atoms in liquid helium [7] made us revisit the subject, since the collective degrees of freedom in the liquid phase (sound waves in the liquid consisting of the neutral  $^4\text{He}$  atoms) provide a new mechanism for shifting and broadening the atomic spectra, in addition to those investigated in gaseous helium. We expected, however, that collisions of the neutral  $\bar{p}\text{He}^+$  atom with the neighboring neutral  $^4\text{He}$  atoms give the dominant contribution to the shift and broadening, both in the gaseous and liquid helium targets. The reason was that the characteristic changes of the  $\bar{p}\text{He}^+$  energy levels due to these collisions are a few orders of magnitude greater than the typical energy of the sound phonons associated with the momentum transfer between the laser photons and the liquid. In the mean time, we neglected the effects of inelastic collisions of  $\bar{p}\text{He}^+$  with  $^4\text{He}$  atoms since the typical thermal collision energies  $\varepsilon_T$  of the order of  $10^{-4}$ – $10^{-3}$  eV are much smaller than the separation  $|\Delta\varepsilon| \gtrsim 0.1$  eV between the energy levels of states with adjacent values of the quantum numbers. The detailed calculations of the collisional quenching rate of antiprotonic helium in [8] show that collisional quenching is indeed strongly suppressed, in agreement with experimental data.

We focus on the transitions  $|i\rangle = (n, \ell) = (39, 35) \rightarrow |f\rangle = (n', \ell') = (38, 34)$  (transition I) and  $(37, 34) \rightarrow (36, 33)$  (transition II), which are of major interest for the experimentalists [2]. For transition I, the corresponding photon wavelength equals  $\lambda_0 = 5972.570$  Å [4] and the resonance energy is  $E_0 = 2.07589$  eV. The natural width  $\Gamma_n$  is determined by the Auger decay rate  $R_A$  of the final state

$$\Gamma_n = \hbar/\tau_n \approx \hbar R_A. \quad (1)$$

For this line, the experimental rate is  $R_A \approx 1.11 \times 10^8 \text{s}^{-1}$  [9] and therefore  $\Gamma_n \approx 0.73 \times 10^{-7}$  eV, the corresponding frequency is  $\nu_n \approx 0.018$  GHz, and the lifetime  $\tau_n = 9.0$  ns. In the case of transition II, the analogous parameters are:  $\lambda_0 = 4707.220$  Å [4],  $E_0 = 2.63392$  eV,  $R_A \approx 2.2 \times 10^8 \text{s}^{-1}$  [10],  $\Gamma_n \approx 1.4 \times 10^{-7}$  eV,  $\nu_n \approx 0.035$  GHz, and  $\tau_n = 4.5$  ns.

In Sec. II we report the estimations of the line shift and broadening due to the collective motion in liquid  $^4\text{He}$ , using the Van Howe formalism [11]. In Sec. III, we evaluate the line shift due to collisions of  $\bar{p}\text{He}^+$  with  $^4\text{He}$  atoms by making use of the quasistatic limit of the results of Ref. [5] in a form that allows for exploiting the experimental data on the pair correlation function in liquid  $^4\text{He}$ . Unfortunately, this method cannot be extended to the evaluation of the line broadening. Section IV includes a brief discussion of the results.

## II. LINE SHIFT AND BROADENING DUE TO THE COLLECTIVE DYNAMICS OF LIQUID HELIUM

In this section, the contributions the line shift and broadening due to the dynamics of liquid  $^4\text{He}$  are estimated in terms of the quantum-mechanical response function  $\mathcal{S}(\mathbf{q}, \omega)$ , which was introduced by Van Hove [11] and discussed in detail for various targets in many textbooks (see e.g., Ref. [12]). The quantities  $\hbar\omega$  and  $\hbar\mathbf{q}$  denote, respectively, the energy and momentum transfers to a given target. The response function depends on the target properties at a fixed temperature and density. On the other hand,  $\mathcal{S}(\mathbf{q}, \omega)$  is independent of the nature of interaction of an impinging particle with the target.

The influence of liquid  $^4\text{He}$  dynamics on the line shift and broadening can be estimated using the method developed by Singwi and Sjölander [13] for describing the  $\gamma$  quantum absorption or emission by a nucleus located in a condensed target. According to Ref. [13], the cross section  $\sigma$  for photon absorption or emission can be expressed in the simplified form

$$\sigma(E) = \frac{\mathcal{A}}{\hbar} \mathcal{S}_i(q, \omega), \quad (2)$$

when the natural resonance width  $\Gamma_n$  is so small that the analogous cross section  $\sigma_0$  for the nucleus set at a fixed position can be approximated by the  $\delta$ -function profile

$$\sigma_0(E) = \mathcal{A} \delta(E - E'_0), \quad (3)$$

in which  $\mathcal{A}$  represents the strength of the resonance,  $E$  is the energy of an absorbed or emitted photon, and  $E'_0$  is the resonance energy. The function  $\mathcal{S}_i(q, \omega)$  denotes the Van Hove single-particle response function, which is the incoherent fraction of the total response function  $\mathcal{S}(q, \omega)$ . In the case of laser-stimulated transitions in the antiprotonic helium

$$\hbar q = p, \quad \hbar\omega = E - E'_0, \quad (4)$$

where  $p$  is the absolute value of momentum of the absorbed or emitted photon. The resonance energy  $E'_0 = E_0 + \Delta E_0$  includes here the line shift  $\Delta E_0$  due to the pairwise interaction. Since  $\Delta E_0 \ll E_0$  in liquid helium, as shown in Sec. III, one can take  $E'_0 \approx E_0$  in numerical estimates of the collective effects.

In the case of a perfect gas, a harmonic solid, or a particle diffusing in a classical fluid according to the Langevin equation, the response function can be rigorously derived [11]. However, an exact form of the response function in normal fluid (He I) and superfluid helium (He II) is not known yet. Therefore,  $\mathcal{S}(q, \omega)$  for liquid helium is usually expressed in terms of simple analytical functions, such as the Gaussian or Lorentzian function, with several parameters to be determined in experiments. Extensive measurements of the response function for liquid helium at various conditions were performed for many years, using x-ray and neutron scattering. The experimental data are available only for the momentum transfers  $q \gtrsim 0.1 \text{ \AA}^{-1}$ . In the case of the  $\bar{p}^4\text{He}^+$  atom, the characteristic momentum transfer equals  $q = p/\hbar = 2\pi/\lambda_0$ , which gives  $q = 0.0011 \text{ \AA}^{-1}$  for transition I and  $q = 0.0013 \text{ \AA}^{-1}$  for transition II. This is two orders of magnitude smaller than in the case of neutron-scattering experiments. Nevertheless, some conclusions can be drawn using the available analytical models and experimental parameters. It is well known from theory and experiment that the response function for liquid  $^4\text{He}$  contains contributions from one-phonon and multiphonon

processes. A dispersion relation for low-energy phonons in superfluid  ${}^4\text{He}$  was first proposed by Landau [14, 15]

$$\omega_{\text{pho}} = c_s q_{\text{pho}}, \quad (5)$$

in which  $\omega_{\text{pho}}$  is the phonon energy,  $q_{\text{pho}}$  denotes the phonon momentum and  $c_s$  represents the sound velocity in the target. Therefore, the interaction of a photon with a  $\bar{p}{}^4\text{He}^+$  atom located in liquid  ${}^4\text{He}$  can lead to the simultaneous creation or annihilation of phonons with the small energy  $E_{\text{pho}}$

$$E_{\text{pho}} = \hbar c_s q = c_s p = hc_s/\lambda. \quad (6)$$

The photon wavelength  $\lambda$  includes here the line shift due to the pairwise potential.

For many years, a sharp one-phonon peak observed in the experimental response function at low temperatures was ascribed to the superfluid fraction of liquid  ${}^4\text{He}$ . This fraction is connected with the presence of the Bose condensate. Therefore, such a peak was expected to disappear above the phase-transition temperature  $T_\lambda = 2.17$  K [16]. However, the further extensive measurements at  $q \approx 0.4 \text{ \AA}^{-1}$  [17–19] proved that the well-defined one-phonon peak does not disappear at  $T > T_\lambda$ . This peak was then ascribed to the collective zero-sound mode, which is independent of the presence of superfluidity. A similar mode is observed in various classical liquids, at sufficiently low  $q$ . Since the laser spectroscopy of antiprotonic helium is characterized by very low momentum transfers, the collective-mode contributions to the line shift and broadening in the He I region are also determined by this acoustic one-phonon process.

The low- $q$  phonon processes in liquid  ${}^4\text{He}$  are well described by the following phenomenological one-phonon response function [17, 18]

$$\mathcal{S}_1(q, \omega) = \frac{\hbar}{\pi} [n_{\text{B}}(\omega, T) + 1] Z(q, T) \left[ \frac{\Gamma_1(q, T)}{\hbar^2 [\omega - \omega_{\text{pho}}(q, T)]^2 + \Gamma_1^2(q, T)} - \frac{\Gamma_1(q, T)}{\hbar^2 [\omega + \omega_{\text{pho}}(q, T)]^2 + \Gamma_1^2(q, T)} \right], \quad (7)$$

in which  $n_{\text{B}}$  is the Bose factor for phonons

$$n_{\text{B}}(\omega, T) = [\exp(\beta_T \omega) - 1]^{-1}, \quad \beta_T = (k_{\text{B}} T)^{-1} \quad (8)$$

and  $k_{\text{B}}$  is the Boltzmann constant. The one-phonon intensity is denoted here by  $Z(q, T)$  and  $\Gamma_1(q, T)$  represents the half width at half maximum of the one-phonon peak. Equation (7) includes both the one-phonon creation and annihilation. The experimental functions  $Z(q, T)$ ,  $\omega_{\text{pho}}(q, T)$ , and  $\Gamma_1(q, T)$  for the saturated vapor pressure (SVP) are presented in Ref. [18] ( $q = 0.4 \text{ \AA}^{-1}$ ) and Ref. [19] ( $q = 0.22 \text{ \AA}^{-1}$ ). In general, for such values of  $q$ , these parameters are insensitive to the phase transition from He II to He I. The phonon energy  $\omega_{\text{pho}}$  practically does not change with temperature in superfluid helium and in the vicinity of  $T_\lambda$ . The same is true for the peak intensity  $Z(q, T)$ . The width  $\Gamma_1$  rises exponentially with rising temperature below  $T \lesssim 2.3$  K and there is no abrupt change at  $T_\lambda$ . The smallest width reported for  $q = 0.4 \text{ \AA}^{-1}$  [18] is on the order of 1 GHz at about 1 K. However, this result is entangled with the experimental energy resolution of 20 GHz, which is taken into account using a convolution of the function (7) with the Gaussian that describes the resolution. The more accurate and reliable measurements [20] using the neutron spin echo techniques give  $\Gamma_1 < 1$  GHz at 1.35 K, for  $q = 0.4 \text{ \AA}^{-1}$ . A similar result is reported in Ref. [21]. For

$T \gtrsim 2.3$  K, the width  $\Gamma_1(q = 0.4 \text{ \AA}^{-1})$  increases slowly from 40 to 70 GHz at  $T \approx 4$  K. Let us note that the observed behavior of  $\Gamma_1$  as a function of temperature is connected with increasing randomness of the considered system (see e.g., Ref. [22] and references therein).

In the antiprotonic helium case, the momentum transfers are smaller by a factor of 220–400 than the lowest experimental  $q$  from Refs. [18–21]. Thus, the knowledge on the behavior of  $\Gamma_1$  as a function of small  $q$  is very important. The experimental data presented in Ref. [19] show that  $\Gamma_1$  linearly decreases towards very small values with decreasing  $q$ , for  $q \lesssim 0.7 \text{ \AA}^{-1}$ . This is consistent with theory which predicts that the one-phonon peak has the  $\delta$ -function profile and  $\Gamma_1 \rightarrow 0$ , in the limit  $q \rightarrow 0$ . Using the linear proportionality and the above-mentioned experimental data, one obtains  $\Gamma_1 < 10^{-2}$  GHz for  $T \lesssim 1$  K. Above this temperature,  $\Gamma_1$  exponentially rises to 0.1 GHz at 2.3 K and then slowly increases to about 0.18 GHz at 4 K.

Since in the antiprotonic-helium experiments  $\beta_T \omega = \beta_T \omega_{\text{pho}} \sim 10^{-2} \ll 1$ , the phonon population factor  $n_B(\omega, T) + 1$  in Eq. (7) approximately equals  $1/(\beta_T \omega)$  for the phonon creation and  $-1/(\beta_T \omega)$  for phonon annihilation. As a result, assuming that  $\mathcal{S}_i(q, \omega) \approx \mathcal{S}_1(q, \omega)$  is a reasonable approximation, the total photon cross section (2) can be expressed as follows

$$\sigma(E) = \frac{\mathcal{A}}{\pi} \frac{Z(q, T)}{\beta_T \omega} \left[ \frac{\Gamma_1}{[E - (E'_0 + E_{\text{pho}})]^2 + \Gamma_1^2} + \frac{\Gamma_1}{[E - (E'_0 - E_{\text{pho}})]^2 + \Gamma_1^2} \right]. \quad (9)$$

Thus, the resonance line is split into the two lines, which are characterized by the line shifts  $\Delta E_1 = E_{\text{pho}}$  and  $-E_{\text{pho}}$ .

The absolute values of the line shifts  $|\Delta E_1| = E_{\text{pho}}$ , which were calculated using Eq. (6), are shown in Table I as functions of temperature. The velocities  $c_s(T)$  at SVP were taken

TABLE I: The absolute values of line shift  $\Delta E_1$  in superfluid and fluid  $^4\text{He}$  at SVP as functions of temperature.

Temperature [K]	Line shift [GHz]	
	Line I	Line II
1.20	0.40	0.50
1.50	0.39	0.50
1.75	0.39	0.49
2.00	0.39	0.48
2.17	0.36	0.46
2.20	0.37	0.47
2.50	0.37	0.47
3.60	0.35	0.44
4.00	0.32	0.40
4.22	0.30	0.38

from Ref. [23] for He II and from Ref. [24] for He I. As it was observed in experiments, the calculated phonon energies do not significantly change in He II and in the vicinity of  $T_\lambda$ . The calculated ratio  $\Gamma_1/|\Delta E_1|$  equals about 0.02 at  $T \approx 1$  K and increases to about 0.5 at 4 K.

### III. COLLISIONAL SHIFT OF RESONANCE LINES

In Refs. [5, 25] the density shift and broadening of the spectral lines of antiprotonic helium atoms in gaseous helium were evaluated in the frame of the semiclassical approach of P.W. Anderson [26]. In this approach the emitter — the antiprotonic atom — is subject to full scale quantum treatment, while the perturber — the ordinary helium atom — evolves classically. The very good agreement of the theoretical results of Refs. [5, 25] with the experimental data taken at a broad range of helium gas densities up to 127 g/l should be attributed to (1) the use of an accurate pair-wise state-dependent potential for the interaction of antiprotonic and ordinary helium atoms, calculated *ab initio* with the symmetrized Rayleigh-Schrödinger theory [6]; (2) the use of curvilinear classical trajectories of the perturbers determined by the interaction potential for the *initial state* of the transition; and (3) the fact that the conditions which justify the impact approximation and the approximation of binary collisions — typical collision duration smaller by an order of magnitude than the average interval between collisions, emitter excitation energies much larger than the thermal collision energies, uncorrelated motion of the perturbers, etc. — are satisfied for the densities and temperatures in consideration. In liquid helium, however, the target density may be still higher, the motion of helium atom cannot be considered as uncorrelated, and this approach cannot be applied. We therefore put the results of Ref. [5] in a form that allows us to use phenomenological data about the liquid helium target density instead of the theoretical calculations, and this way we obtain a reliable estimate of the collisional shift of the spectral lines. Unfortunately, the line broadening cannot be evaluated this way since similar naive approaches are known to produce wrong values, as pointed out in Ref. [22].

In the semiclassical approach, the density shift  $\Delta E_0$  of the resonance energy  $E_0$  of the transition  $|i\rangle \rightarrow |f\rangle$  between the initial and final quantum states of the antiprotonic atom, due to the interaction with the atoms of the surrounding helium gas, is given by

$$\Delta E_0 = N_0 \left\langle 2\pi v \int db b \sin \left( \int dt \Delta V(\mathbf{R}_b(t)) \right) \right\rangle_v. \quad (10)$$

Here  $N_0$  is the number density of the helium gas,  $N_0 = \varrho/M_{\text{He}}$ ,  $\varrho$  being the target density and  $M_{\text{He}}$  being the  ${}^4\text{He}$ -atom mass;  $\Delta V(\mathbf{r}) = V_f(\mathbf{r}) - V_i(\mathbf{r})$  is the difference of the state-dependent  $\bar{p}^4\text{He}^+$ -He interaction potentials;  $\mathbf{R}_b(t)$  is the classical trajectory of a He atom with impact parameter  $b$ , determined by the interaction potential in the *initial* state and parametrized with the proper time  $t$ ; and  $\langle \dots \rangle_v$  denotes averaging over the Maxwell-distributed asymptotic velocities  $v$  of the helium atom. Equation (10) has been derived in the approximation of an ideal helium gas, pairwise  $\bar{p}^4\text{He}^+$ -He interaction, and under a few more assumptions discussed in detail in Ref. [5]. At low target temperatures, kinetic energy of most of the incident helium atoms is small, and also small is the phase accumulated along a typical trajectory

$$\eta_b = \int dt \Delta V(\mathbf{R}_b(t)) \ll 1, \quad (11)$$

so that  $\sin \eta_b \approx \eta_b$ . We can then transform Eq. (10) to the following form

$$\Delta E_0 = \int d^3r \rho(\mathbf{r}) [V_f(\mathbf{r}) - V_i(\mathbf{r})], \quad (12)$$

where

$$\rho(\mathbf{r}) = 2\pi N_0 \left\langle \int db b \int dt \delta(\mathbf{r} - \mathbf{R}_b(t)) \right\rangle_v. \quad (13)$$

For spherically symmetric  $V_{i,f}(\mathbf{r}) = V_{i,f}(r)$ ,  $\rho$  is also symmetric:  $\rho(\mathbf{r}) = \rho(r)$ . Equation (12) has a simple physical interpretation: due to the interaction with a helium atom at position  $\mathbf{r}$ , the energy levels of the initial and final states of  $\bar{p}^4\text{He}^+$  (placed at the origin) are shifted by  $V_{i,f}(\mathbf{r})$ , respectively, and the transition energy is shifted by their difference. The observable shift is the average of the latter over the spatial distribution  $\rho(\mathbf{r})$  of the surrounding helium atoms. This approximation will be referred to as “quasistatic limit”.

Equation (12) may be the starting point for a self-consistent approximate evaluation of the density shift, provided that the helium gas density  $\rho(\mathbf{r})$  is known. One could think of three different estimates of  $\rho(\mathbf{r})$ :

1. The helium gas density  $\rho_c(r)$  calculated from the classical trajectories used in Ref. [5] is one estimate. Equation (13) gives the algorithm of calculating  $\rho_c(r)$  from the set of classical trajectories. The corresponding curve for a temperature of 5.4 K, renormalized to 1 at  $r = 10 \text{ \AA}$ , is shown in Fig. 1. [The curliness of  $\rho_c$  is due to the too rough discretization of the integrals in Eq. (13)].
2. Another estimate is the helium gas density  $\rho_q(r)$  equal to the modulus squared of the two-body scattering wave function for the system of point-like helium and  $\bar{p}^4\text{He}^+$  atoms interacting via the potential in the initial state  $V_i(r)$ . For a comparison, in Fig. 1 we plot  $\rho_q(r)$  evaluated <sup>1</sup> for the helium temperature  $T = 5.8 \text{ K}$  and renormalized to 1 at  $r = 10 \text{ \AA}$  [27].
3. A third estimate is the helium gas density  $\rho_{\text{exp}}(r)$  from experiment. Of course, there are no data on the helium density in the neighborhood of an  $\bar{p}^4\text{He}^+$  atom, but as a first approximation one can use the static pair correlation function  $g(\mathbf{r}, T)$  for pure helium that gives the probability density of finding a helium atom located at  $\mathbf{r}$  if the reference particle is placed at the origin. At large  $r$ ,  $g(\mathbf{r}, T) \rightarrow 1$ . Isotropic media, such as liquid helium, can be described using the radial function  $\rho_{\text{exp}}(r) = g(r, T)$ . The pair correlation function is usually determined by means of x-ray or neutron scattering.

In the present work we evaluate the collisional line shift using Eq. (12) and the phenomenological density  $\rho_{\text{exp}}(r)$  extracted from the set of functions  $g(r, T)$  of Ref. [28] which were determined for fluid and superfluid  $^4\text{He}$  at the saturated vapor pressure and various temperatures. We make no use of  $\rho_c(r)$  or  $\rho_q(r)$  since they have been calculated under assumptions that may not be valid in liquid helium; any partial results obtained with  $\rho_c(r)$  or  $\rho_q(r)$  are listed uniquely for comparison. The functions  $g(r, T)$  for temperatures  $T = 1.77$  and  $4.27 \text{ K}$  are plotted in Fig. 1. This figure shows that the density distributions  $\rho_{\text{exp}}(r)$  in both the fluid and superfluid  $^4\text{He}$  are very close. The helium atoms cannot be closer than about  $2 \text{ \AA}$ . The maxima at about  $3.5$  and  $6.8 \text{ \AA}$  correspond to the first and second shell of neighbors, respectively. The shape of the quantum-mechanical density  $\rho_q(r)$ , plotted for comparison, is very similar, in particular at small distances  $r \lesssim 2.5 \text{ \AA}$ . This proves that radial pair correlation function, which was obtained for a pure  $^4\text{He}$  target, can be applied for calculating the line shift with the help of Eq. (12). At distances  $r \gtrsim 2.5 \text{ \AA}$ , the difference between the functions  $g(r, T)$  and  $\rho_q(r)$  increases. This is due to the increasing role of many-atom interactions which are not taken into account in  $\rho_q(r)$ , while the experimental  $\rho_{\text{exp}}(r)$  describes the real structure of the quantum liquid  $^4\text{He}$ .

---

<sup>1</sup> The details of the calculation will be presented in a separate paper

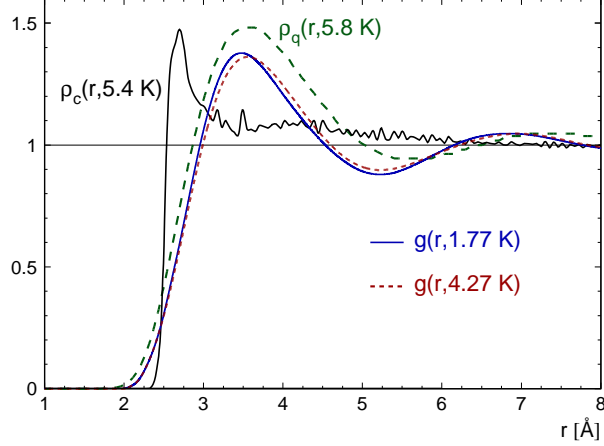


FIG. 1: (Color online) The experimental functions  $g(r, T)$  for liquid  ${}^4\text{He}$  at SVP and  $T = 1.77$  and  $4.27$  K [28], together with the classical  $\rho_c(r)$  and quantum-mechanical  $\rho_q(r)$  probability densities which were calculated in the two-particle approximation [27]. To emphasize the similarity of their shape, the curves  $\rho_c(r)$  and  $\rho_q(r)$  in the plot have been *renormalized* to unit radial density at  $r = 10$  Å.

The potential curves  $V_{(n,\ell)}(r)$ ,  $V_{(n',\ell')}(r)$ , and  $\Delta V(r)$ , together with the correlation functions [28], are shown in Fig. 2 for transition I. One can see that the main contribution to

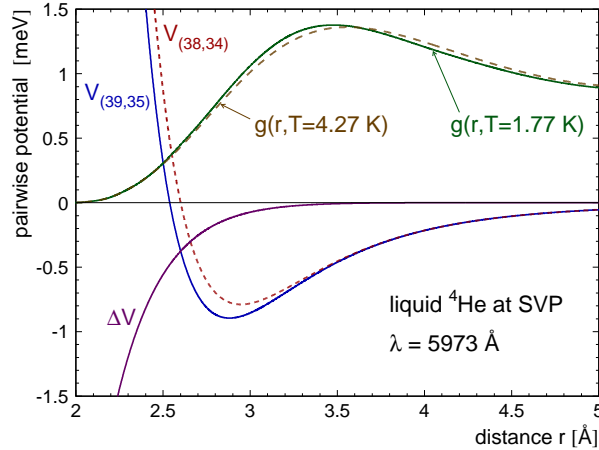


FIG. 2: (Color online) The pairwise potential curves  $V_{(n,\ell)}(r)$ ,  $V_{(n',\ell')}(r)$ , and  $\Delta V(r)$  for transition I, together with the pair correlation function  $g(r, T)$  at  $1.77$  K and  $4.27$  K [28], versus the distance  $r$  between the antiprotonic helium and the  ${}^4\text{He}$  atom.

the resonance energy shift Eq. (12) comes from the interval  $2.2 \gtrsim r \lesssim 3.4$  Å, where both the  $\Delta V(r)$  and  $\rho_{\text{exp}}(r) \equiv g(r, T)$  have significant magnitudes.

In order to check the validity of using the pairwise interaction potentials for the determination of resonance shifts, in Fig. 3 we plot the average number  $n(r)$  of  ${}^4\text{He}$  atoms that are located within the sphere of radius  $r$

$$n(r) = 4\pi N_0 \int_0^r dr' r'^2 \rho_{\text{exp}}(r'), \quad (14)$$



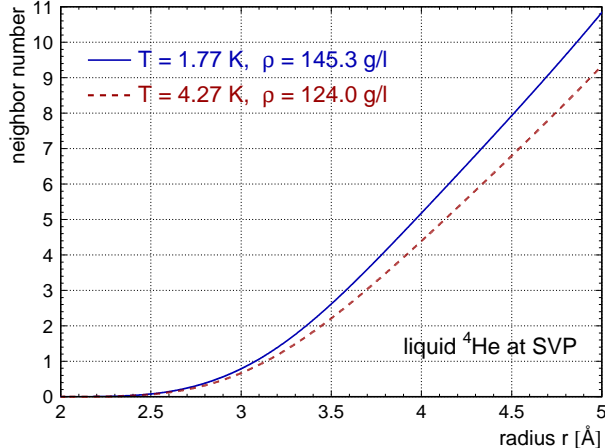


FIG. 3: (Color online) The number  $n(r)$  of  ${}^4\text{He}$  atoms within the sphere of radius  $r$  that surround an atom placed at  $r = 0$  in liquid helium.

for  $T = 1.77$  and  $4.27$  K at SVP. The plot shows that  $n(r) \leq 1$  for  $r \leq 3.1$ – $3.2$  Å, depending on the target density. Since  $\Delta V(r)$  has the largest absolute values within this interval of  $r$ , one can expect that Eq. (12) establishes a good approximation to the resonance shifts.

The number density  $N_0$  in Eq. (13) is a factor that suggests a direct proportionality of the energy shift with respect to the helium density. However, the function  $\rho_{\text{exp}}(r) = g(r, T)$  slightly varies with temperature and thus also with the density, which at SVP is determined by temperature. Therefore, the integration in Eq. (12) leads to a higher-order correction to the above-mentioned linear proportionality.

The resonance line shifts, which were calculated in the quasistatic limit using the experimental helium density  $\rho_{\text{exp}}(r) \equiv g(r, T)$  from Ref. [28], are shown in Table II for the temperature interval  $T = 1.0$ – $4.27$  K at SVP. The corresponding  ${}^4\text{He}$  densities are interpolated with the help of data from Ref. [29]. Although transition II was not observed at gas densities higher than  $32$  g/l [4], the calculated resonance shifts are also given here for this line, for the sake of comparison. Note that there are no experimental data about the line shift and broadening in liquid helium. The density effects have been studied experimentally only in a gaseous helium target at pressures  $0.2$ – $8.0$  bars, temperatures  $5.8$ – $6.3$  K and target densities ranging from about  $1.4$  to  $127$  g/l [4, 30] where the linear dependence on the target density has been confirmed within the experimental accuracy. The recent experimental results of Ref. [30] read  $\Delta E_0/\rho = -0.63 \pm 0.03$  GHz·g/l for transition I and  $\Delta E_0/\rho = -0.21 \pm 0.02$  GHz·g/l for transition II. Table II shows that the values of the reduced shift  $|\Delta E_0|/\rho$  in liquid  ${}^4\text{He}$ , calculated using the phenomenological  $\rho_{\text{exp}}(r)$ , differ from both the experimental data and the semiclassical calculations for gaseous  ${}^4\text{He}$ .

The reduced resonance redshifts  $|\Delta E_0|/\rho$  as functions of the upper limit  $r_{\text{max}}$  of the integral Eq. (12) are plotted in Fig. 4. In the case of line I, the asymptotic value of  $\Delta E_0$  is already reached at  $r_{\text{max}} \approx 3.8$  Å. This confirms that the approximation of binary interactions is a good one in this case. A better approximation would be possible when the three-body interaction potentials are calculated, which is a much more complicated task. For line II, the asymptotic value of  $\Delta E_0$  is achieved only at  $r_{\text{max}} \approx 9$  Å since  $\Delta V(r)$  changes sign at  $r = 3.3$  Å and  $\Delta E_0(r_{\text{max}})$  is not a monotonic function. Thus, in this particular case, the binary interaction approximation is not as good as for line I.

TABLE II: The line shift  $\Delta E_0$  [GHz] and the reduced line shift  $\Delta E_0/\rho$  [GHz.l/g] for liquid  ${}^4\text{He}$  at SVP, calculated with Eq. (12) using  $g(r, T)$  from Ref. [28]. For comparison, in the last two columns are given the values of the reduced line shift in gaseous helium, calculated in the semi-classical approach of Ref. [5].

Temperature [K]	Density [g/l]	$\Delta E_0$		$\Delta E_0/\rho$		$\Delta E_0/\rho$ in ${}^4\text{He}$ gas	
		Line I	Line II	Line I	Line II	Line I	Line II
1.00	145.1	-64.1	-37.7	-0.442	-0.260	-0.509	-0.181
1.38	145.1	-70.2	-43.7	-0.484	-0.301		
1.77	145.3	-63.1	-36.9	-0.434	-0.254		
1.97	145.6	-64.3	-37.8	-0.442	-0.260		
2.07	145.8	-67.5	-40.9	-0.463	-0.280		
2.12	145.9	-64.4	-37.8	-0.442	-0.259		
2.15	146.0	-67.0	-40.3	-0.459	-0.276		
2.27	145.9	-62.3	-35.7	-0.427	-0.245		
3.00	141.2	-61.0	-35.3	-0.432	-0.250	-0.582	-0.203
3.60	134.8	-58.1	-33.6	-0.431	-0.249	-0.591	-0.208
4.27	124.0	-53.3	-30.9	-0.429	-0.249		

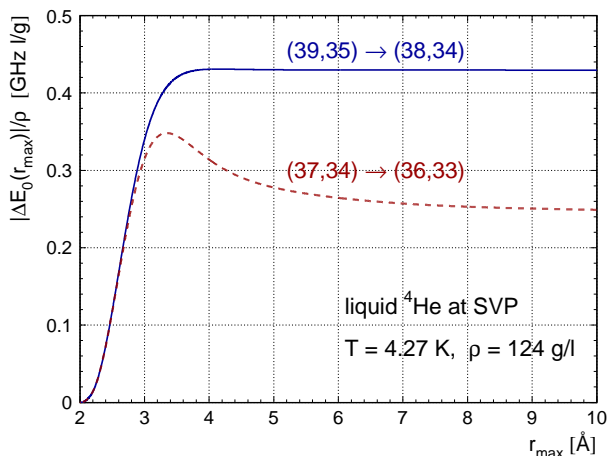


FIG. 4: (Color online) The reduced resonance redshifts  $|\Delta E_0|/\rho$  for transition I and II as functions of  $r_{\max}$  for  $g(r, 4.27 \text{ K})$  from Ref. [28].

#### IV. CONCLUSIONS

The present work was motivated by the attempts of the ASACUSA collaboration at CERN for the high-accuracy spectroscopy measurements of the antiprotonic helium atoms in liquid helium media, where the broadening and shift of the spectral lines due to the collective many-body effects had not been investigated.

The resonance line shift of the antiprotonic helium atom located in liquid  ${}^4\text{He}$  is the sum of the contribution  $\Delta E_0$  from the pairwise  $\bar{p}\text{He}^+ - {}^4\text{He}$  interaction and the contribution  $\Delta E_1$  due to the collective dynamics of the liquid. The shift  $\Delta E_0$  gives a correction on the order of  $|\Delta E_0|/E_0 \sim 10^{-4}$  to the resonance wavelength  $\lambda_0$  of an isolated  $\bar{p}\text{He}^+$  atom. The

correction due to the collective dynamics is much smaller,  $|\Delta E_1|/E_0 \sim 10^{-6}$  but still may be of importance for high-precision measurements.

The calculated values of  $\Delta E_0/\rho$  in Table II exhibit appreciable variations (9% for line I) with changing temperature, for  $T < 2.27$  K and almost constant density. Thus, this phenomenon is apparent only in superfluid  $^4\text{He}$ . At higher temperatures, where  $^4\text{He}$  density at SVP significantly decreases,  $\Delta E_0/\rho$  is practically constant. A similar effect was observed in the experiments using gaseous helium targets [4, 30].

The reduced line width  $\Gamma_1/\rho$  that comes from the collective motion in liquid  $^4\text{He}$  ranges from about  $10^{-4}$  to  $10^{-3}$  GHz·l/g. Thus, the corresponding contribution to the line broadening is much lower than the collisional broadening in a gaseous helium target as reported in Ref. [5]. As already pointed out, our method for the evaluation of the density shift in the quasistatic limit using phenomenological data about the helium target density cannot be applied in calculating the collisional line broadening, and we only can estimate the broadening in a gaseous helium target as an upper limit for the broadening in liquid helium.

The accuracy of the calculated quasistatic line shifts and broadening could be improved if the potentials of the  $\bar{p}\text{He}^+$  interaction with two helium atoms were available. However, the calculation of such potentials is much more complicated than in the case of pairwise potential.

Note that one of the methods of studying liquid-helium structure is the observation of foreign atoms and ions implanted in a liquid  $^4\text{He}$  target. Unfortunately, the presence of such an atom strongly affects its helium vicinity. A large cavity is created around the foreign atom, due to the Pauli repulsion between the electrons in this atom and the surrounding helium atoms (see e.g., Ref. [31]). The antiprotonic helium atom, in contrast, having only one electron in the 1s state, is a good candidate for such studies, as is indicated by the similarity of the densities  $\rho_{\text{exp}}(r) \equiv g(r, T)$  and  $\rho_q(r)$ .

## Acknowledgments

We would like to thank M. Hori and A. Sótér for the valuable discussions. This work has been performed under the framework of collaboration between the Bulgarian Academy of Sciences and Polish Academy of Sciences.

- 
- [1] T. Yamazaki, N. Morita, R. Hayano, E. Widmann, and J. Eades, *Phys. Rep.* **366**, 183 (2002).
  - [2] M. Hori, A. Sótér, D. Barna, et al., *Nature* **475**, 484 (2011).
  - [3] T. Pask, D. Barna, A. Dax, et al., *Phys. Lett. B* **678**, 55 (2009).
  - [4] H. A. Torii, R. S. Hayano, M. Hori, et al., *Phys. Rev. A* **59**, 223 (1999).
  - [5] D. Bakalov, B. Jeziorski, T. Korona, K. Szalewicz, and E. Tchukova, *Phys. Rev. Lett.* **84**, 2350 (2000).
  - [6] B. Jeziorski and K. Szalewicz, in *Encyclopedia of Computational Chemistry*, edited by P. von Ragué et al. (Wiley, Chichester, UK, 1998).
  - [7] M. Hori, private communication.
  - [8] B. D. Obreshkov, D. D. Bakalov, B. Lepetit, and K. Szalewicz, *Phys. Rev. A* **69**, 042701 (2004).
  - [9] H. Yamaguchi, T. Ishikawa, J. Sakaguchi, et al., *Phys. Rev. A* **66**, 022504 (2002).

- [10] M. Hori, H. A. Torii, R. S. Hayano, et al., Phys. Rev. A **57**, 1698 (1998).
- [11] L. Van Hove, Phys. Rev. **95**, 249 (1954).
- [12] S. W. Lovesey, *Theory of Neutron Scattering from Condensed Matter* (Clarendon Press, Oxford, 1984).
- [13] K. S. Singwi and A. Sjölander, Phys. Rev. **120**, 1093 (1960).
- [14] L. Landau, Phys. Rev. **60**, 356 (1941).
- [15] L. Landau, J. Phys. USSR **5**, 71 (1941).
- [16] A. D. B. Woods and E. C. Svensson, Phys. Rev. Lett. **41**, 974 (1978).
- [17] E. F. Talbot, H. R. Glyde, W. G. Stirling, and E. C. Svensson, Phys. Rev. B **38**, 11229 (1988).
- [18] W. G. Stirling and H. R. Glyde, Phys. Rev. B **41**, 4224 (1990).
- [19] I. V. Bogoyavlenskii, A. V. Puchkov, and A. N. Skomorokhov, Low Temp. Phys. **30**, 745 (2004).
- [20] F. Mezei and W. G. Stirling, in *75th Jubilee Conference on Helium-4*, edited by J. G. M. Armitage (World Scientific, Singapore, 1983).
- [21] S. Klimko, C. Stadler, P. Böni, et al., Physica B **335**, 188 (2003).
- [22] S. Alexiou, High Energy Density Physics **5**, 225 (2009).
- [23] J. Maynard, Phys. Rev. B **14**, 3868 (1976).
- [24] J. C. Findlay, A. Pitt, H. Grayson Smith, and J. O. Wilhelm, Phys. Rev. **54**, 506 (1938).
- [25] D. Bakalov, Hyperfine Interact. **209**, 25 (2012).
- [26] P. Anderson, Phys. Rev. **86**, 809 (1952).
- [27] D. Bakalov, B. Obreshkov, B. Jeziorski, T. Korona, and K. Szalewicz, unpublished.
- [28] V. F. Sears et al., Tech. Rep. AECL-6779, Atomic Energy of Canada Limited (1979).
- [29] R. J. Donnelly and C. F. Barenghi, J. Phys. Chem. Ref. Data **27**, 1217 (1998).
- [30] M. Hori, A. Dax, J. Eades, et al., Phys. Rev. Lett. **96**, 243401 (2006).
- [31] D. Mateo, A. Hernando, M. Barranco, R. Mayol, and M. Pi, Phys. Rev. B **83**, 174505 (2011).